

## Variation in chemical composition of Asian dusts on Jeju Island related to their inflow pathways during 2010-2015

Jung-Min Song<sup>1</sup>, Jun-Oh Bu<sup>1</sup>, Hee-Jung Ko<sup>2</sup>, Won-Hyung Kim<sup>1</sup>, and Chang-Hee Kang<sup>1,★</sup>

<sup>1</sup>Department of Chemistry and Cosmetics, Jeju National University, Jeju 63243, Korea

<sup>2</sup>Environmental Meteorology Research Division, National Institute of Meteorological Sciences, Jeju 63568, Korea

(Received February 6, 2017; Revised June 14, 2017; Accepted June 14, 2017)

**Abstract** In order to examine the variation characteristics of chemical compositions in relation to the inflow pathways of Asian dust, PM<sub>10</sub> and PM<sub>2.5</sub> aerosols were collected at Gosan site of Jeju Island during the Asian dust days between 2010 and 2015, and their chemical compositions were analyzed. The mean mass concentrations of PM<sub>10</sub> and PM<sub>2.5</sub> during Asian dust days were  $130.0 \pm 90.2$  and  $38.2 \pm 24.7$   $\mu\text{g}/\text{m}^3$ , respectively. The composition ratios of major secondary pollutants (nss-SO<sub>4</sub><sup>2-</sup>, NH<sub>4</sub><sup>+</sup>, NO<sub>3</sub><sup>-</sup>) were high as 53.7% for PM<sub>10-2.5</sub> and 90.6% for PM<sub>2.5</sub>. When the Asian dusts had been transported to the Korean Peninsula via Loess Plateau of central China, the concentrations of nss-Ca<sup>2+</sup>, NH<sub>4</sub><sup>+</sup>, nss-SO<sub>4</sub><sup>2-</sup>, and NO<sub>3</sub><sup>-</sup> increased more noticeably. Whereas in case when the inflow pathways of Asian dust had been through the Bohai bay, the concentrations of the crustal species such as Al, Fe, and Ca were relatively high in coarse particles. The atmospheric aerosols were acidified largely by sulfuric and nitric acids. They were neutralized mainly by calcium carbonate in coarse particle mode passed through Manchuria area, but by ammonia in fine particle mode passed through Loess plateau and Bohai bay. Ammonium salts are assumed to exist as ammonium sulfate and ammonium nitrate in coarse particles, but mostly as ammonium sulfate in fine particles.

**Key words:** Asian dust, Transport Pathway, PM<sub>10</sub>, PM<sub>2.5</sub>, Gosan site

### 1. Introduction

Asian dust events occur mainly in the spring season in the Taklamakan Desert of the Tarim Basin located in northwestern China, the Gobi Desert spread across northern China and southern Mongolia, the Kubuchi and Ordos deserts in Inner Mongolia in China, and the Loess Plateau (the Huangtu Plateau) in China. These locations are known to be major

dust sources in Asia.<sup>1-4</sup> About 30% of Asian dust occurring from original sources is redeposited onto other nearby sources, and 20% is transported into neighboring areas, within the interiors of China. The remaining 50% is reported to travel long distances and affects Korea, Japan, the Pacific Ocean, and even the west coast of the United States.<sup>5,6</sup>

Globally, the Sahara Desert in North Africa generates the largest amount of mineral dust, accounting for

★ Corresponding author

Phone : +82-(0)64-754-3545 Fax : +82-(0)64-756-3561

E-mail : changhee@jejunu.ac.kr

This is an open access article distributed under the terms of the Creative Commons Attribution Non-Commercial License (<http://creativecommons.org/licenses/by-nc/3.0>) which permits unrestricted non-commercial use, distribution, and reproduction in any medium, provided the original work is properly cited.

50-70 % of the world's dust.<sup>7,8</sup> However, dust from this region has not directly influenced human activity because it predominantly travels across the Atlantic owing to trade winds. In contrast, the amount of dust emitted from East Asia is relatively low but significantly influences human activities in densely populated areas, such as eastern China, Korea, and Japan, owing to the Westerlies. Research on aerosol species in densely populated areas worldwide has shown that the dust contribution from East Asia is higher than that from the US and Europe.<sup>9</sup>

The Korea Meteorological Administration (KMA) has been conducting a forecasting study on major Asian dust sources and pathways affecting Korea since it initiated the Asian dust warning system in 2002. According to the Asian Dust and Smog Report in 2015," published by the National Institute of Meteorological Research (NIMR) of the KMA, the number of Asian dust events steadily increased from 2002 to 2010, decreased from 2011 to 2013, and has been increasing again since 2014.<sup>10</sup> East Asian dust sources are divided into three regions: Gobi and Inner Mongolia, Manchuria, and the Loess Plateau. The transport pathways are categorized into five routes: Bohai Bay, Manchuria, the Loess Plateau, Liaodong Peninsula, and Shandong Peninsula. The relative contributions of Asian dust sources to Korea have been determined as follows: 81 % from the Gobi Desert and Inner Mongolia, 19 % from Manchuria, and 1 % from the Loess Plateau. That is, the Asian dust affecting Korea is primarily derived from the Inner Mongolia plateau and the Gobi Desert in Mongolia.<sup>10</sup> Approximately 90 % of Mongolia is undergoing desertification, including the southern Gobi Desert. The intensity of desertification is significant, and thus the occurrence and mass of transported Asian dust has been gradually increasing.<sup>11</sup>

Asian dust does have some benefits; it neutralizes acid rain and acidic soils, as it contains alkaline species, and it provides inorganic salts to marine plankton and components, such as magnesium, that expedite plant growth. However, Asian dust can cause plant growth disorders and significant harm to aerospace and precision industries. It can harm

humans by leading to poor visibility events and respiratory and eye diseases, and can also negatively impact precipitation and soil environment. Asian dust particles larger than 20  $\mu\text{m}$  in diameter settle easily, but small particles can remain in the atmosphere and be transported to higher altitudes. Asian dust particles observed in Korea range from 1 to 10  $\mu\text{m}$  in size. Particles smaller than  $\sim 3 \mu\text{m}$  are the most common and affect  $\text{PM}_{10}$  and  $\text{PM}_{2.5}$  aerosols.<sup>12</sup> The contents of organic carbon, water-soluble salts, and toxic heavy metals are different in  $\text{PM}_{10}$  and  $\text{PM}_{2.5}$ , concentrations, depending on the air pollutants emitted from industrial areas in China and their transport pathways into Korea via the Westerlies. The resulting damage from these particles also differs.<sup>13,14</sup>

In this study,  $\text{PM}_{10}$  and  $\text{PM}_{2.5}$  samples were collected from the Gosan site on Jeju Island during Asian dust periods and their chemical compositions analyzed. Based on the analytical results, we examined the pollution characteristics of Asian dust and their effects on air quality on Jeju. In addition, we compared the changes in chemical compositions of atmospheric aerosols depending on the inflow pathways of Asian dusts transported to Jeju Island.

## 2. Experimental

### 2.1. Asian dust sample collection

Asian dust samples of  $\text{PM}_{10}$  and  $\text{PM}_{2.5}$  were collected on Asian dust event days. Samples were obtained 12 times (24-h interval) from 2010-2015 at the Gosan station (33°17' N, 126°10' E) on Jeju Island, Korea. Asian dust samples were classified according to source and transport pathway (Fig. 1):

- Case I was defined by dust originating from the Gobi and Inner Mongolia that flowed to Jeju through Manchuria; this occurred twice and four samples each of  $\text{PM}_{10}$  and  $\text{PM}_{2.5}$  were collected.
- Case II was defined by dust transported through Bohai Bay, which occurred five times and six samples each of  $\text{PM}_{10}$  and  $\text{PM}_{2.5}$  were collected.
- Case III was defined by dust transported through the Loess Plateau, which occurred five times and nine samples each of  $\text{PM}_{10}$  and  $\text{PM}_{2.5}$  were

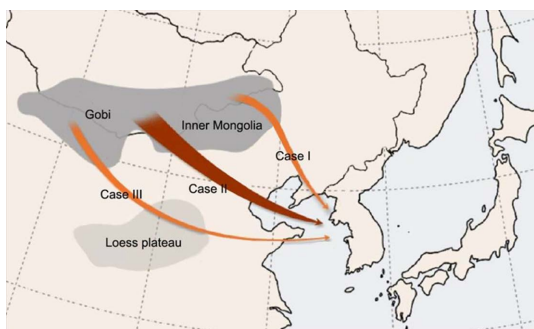


Fig. 1. Classification of main transport pathways of Asian dusts.

collected.

In total, 19 PM<sub>10</sub> and 19 PM<sub>2.5</sub> samples were collected (Table 1).

Samples were collected via Teflon filters (Zefluor™, PTFE 47 μm dia., 2.0 μm pore size, Pall Co., USA) using a PM<sub>10</sub>/PM<sub>2.5</sub> Sequential Air Sampler (PMS-102/PMS-103/PMS-104, APM Engineering, Korea) and PM<sub>2.5</sub> Air Sampler (Model URG-2000-30EH, URG Corporation, USA). The airflow rate of the sampler was maintained at 16.7 L/min using an attached mass flow controller (MFC). The collected samples were sealed in plastic petri dishes (SPL Life Sciences, PS, 52.7 × 12.6 mm) onsite, and then dried in a desiccator (48 to 96 h) until they reached a constant weight. The weight was measured with an accuracy of 0.01 mg. Weighed samples were stored in a freezer maintained at -24 °C until analysis.<sup>15</sup>

## 2.2. Asian dust sample analysis

### 2.2.1. Analyses of ionic species

The PM<sub>10</sub> sample filters were divided in two: one half for ionic species analysis and the other half for elemental species analysis. The entire PM<sub>2.5</sub> sample filter was used for ionic species analysis. Water-soluble ionic species were eluted after placing the collected sample filters in Nalgene bottles (HDPE, 125 mL), adding 0.2 mL of ethanol and 30 mL of ultrapure water (18.2 MΩ), and agitating them in an ultrasonic extractor for 30 min and a shaker for 1 h (200 rpm). After filtering out insoluble species in the eluted sample using a syringe filter (Whatman, PVDF syringe filter, 0.45 μm pore size), the filtrates were analyzed for ionic species concentrations.

The major water-soluble ionic species were determined using ion chromatography (IC), the analysis conditions of which are listed in Table 2. The standard solutions for analyzing major cations (NH<sub>4</sub><sup>+</sup>, Na<sup>+</sup>, K<sup>+</sup>, Ca<sup>2+</sup>, Mg<sup>2+</sup>) were prepared using 100 μg/mL AccuStandards. Here, the linearity of the standard calibration curve using the standard solution diluted to varying concentrations (0.1–5.0 μg/mL) showed that the coefficient of determination (R<sup>2</sup>) was higher than 0.9999. The standard solutions for anions (SO<sub>4</sub><sup>2-</sup>, NO<sub>3</sub><sup>-</sup>, Cl<sup>-</sup>) were prepared using Sigma-Aldrich's primary standard containing 99.999 % (NH<sub>4</sub>)<sub>2</sub>SO<sub>4</sub>, 99.99 % KNO<sub>3</sub>, and 99.99 % NaCl. The standard calibration curve was made using concentrations of the standard solution ranging from 0.1 to

Table 1. Classification of the transport pathways of Asian dusts and sampling dates for the study

Classification	Transport Pathway	Date	No. of Samples
Case I	Gobi/Inner Mongolia → Manchuria → Liaodong Peninsula → Korean Peninsula (Jeju Island)	2015. 2. 22–24,	4 (PM <sub>10</sub> )
		2015. 3. 22	4 (PM <sub>2.5</sub> )
Case II	Gobi/Inner Mongolia → Bohai bay → Korean Peninsula (Jeju Island)	2010. 1. 25,	6 (PM <sub>10</sub> ) 6 (PM <sub>2.5</sub> )
		2010. 5. 10–11	
		2013. 4. 9,	
		2014. 1. 1, 2014. 1. 20	
Case III	Gobi/Inner Mongolia → Loess plateau → Korean Peninsula (Jeju Island)	2010. 3. 20,	9 (PM <sub>10</sub> ) 9 (PM <sub>2.5</sub> )
		2011. 5. 3–4	
		2013. 3. 19,	
		2014. 5. 26–29, 2015. 6. 12	

Table 2. Instrumental conditions for ion chromatography analysis

	Cation	Anion	Organic acid	
IC	Metrohm Modula IC	Metrohm Modula IC	Dionex DX-500	Metrohm Modula IC
Column	Metrosep Cation C4-150 Cation C6-150	Metrosep A-SUPP-5 A-SUPP-16	IonPac AG11/ IonPac AS11	Metrosep A-SUPP-16
Eluent	4.0 mM HNO <sub>3</sub>	1.0 mM NaHCO <sub>3</sub> / 3.2 mM Na <sub>2</sub> CO <sub>3</sub>	0.5 mM NaOH/ 5.0 mM MSA	25.0 mM NaOH/ 3.0 mM Na <sub>2</sub> CO <sub>3</sub>
Suppressor	non-suppressed	Metrohm 753/ 100 mM H <sub>2</sub> SO <sub>4</sub>	Dionex ASRS	Metrohm753/ 200 mM H <sub>2</sub> SO <sub>4</sub>
Flow rate	0.9 mL/min	0.7~0.8 mL/min	1.1 mL/min	1.5 mL/min
Injection Volume	50 µL	50~100 µL	200 µL	100~200 µL

5.0 µg/mL. The standard solutions for trace organic acid ions and HCOO<sup>-</sup>, CH<sub>3</sub>COO<sup>-</sup>, F<sup>-</sup>, and CH<sub>3</sub>SO<sub>3</sub><sup>-</sup> ions were generated using Sigma-Aldrich's primary standard containing NaF (99.99%), CH<sub>3</sub>COONa·3H<sub>2</sub>O (99.9%), HCOONa (99%), and CH<sub>3</sub>SO<sub>3</sub>Na (98%). The concentrations of the standard solutions ranged from 0.01 to 0.5 µg/mL. Correlation of the standard calibration curve for the analysis of anions and organic acids showed good linearity, with R<sup>2</sup> equal to or higher than 0.9999. During the analysis period, and depending on the species, the instrument detection limit (IDL) for the IC analyses ranged from 0.3 to 10.7 µg/mL, and the coefficient of variation (CV) ranged from 0.1 to 3.3%.

#### 2.2.2. Analyses of elemental species

The elemental species of PM<sub>10</sub> and PM<sub>2.5</sub> were analyzed after pretreatment with the microwave acid-digestion method, according to the US EPA's "Compendium of methods for determination of inorganic compounds in ambient air (Method IO-3)".<sup>16</sup> The sample filter was cut into small pieces and placed in a polyfluoroalkoxy (PFA) vessel, and then extracted using a microwave digestion apparatus (STARTD, Milestone, USA) after adding 10 mL of mixed 5.55% HNO<sub>3</sub> and 16.75% HCl acid to the vessel. At this time, the inside of the microwave was irradiated with 1000 W radio frequency power, and the temperature was raised to 180 °C for 15 min, held at this temperature for 15 min, and then cooled

gradually to room temperature. After acid digestion, insoluble parts of the sample solution were filtered with a syringe filter (Whatman, PVDF syringe filter, 0.45 µm pore size). Next, 5 mL of a 3% HNO<sub>3</sub> and 8% HCl mixture was added and then diluted to 25 mL with ultrapure water in a volumetric flask.

Twenty elemental species were analyzed using an ICP-OES (OPTIMA 7300DV, PerkinElmer, USA) and ICP-MS (ELAN DRC-e, PerkinElmer, USA). AccuStandard's 1000 µg/mL standard for ICP and Perkin Elmer's 10 µg/mL standard for ICP/MS were used to prepare the standard solutions for the standard calibration curves for the sample analyses. The standard solutions for the analysis of high concentration species were diluted to 0.01 to 5.0 µg/mL, and those of low concentration species were diluted to 1 to 50 µg/L. For the dilution of standard solutions acid solutions (3% HNO<sub>3</sub>/8% HCl for ICP-OES and 1% HNO<sub>3</sub> for ICP-MS) were used to minimize the matrix effect. The IDLs of the elemental analyses ranged from 0.9 to 18.3 µg/L for ICP-OES and 6.3 to 62.8 ng/L for ICP-MS.

### 3. Results and Discussion

#### 3.1. Chemical compositions of Asian dusts

Asian dusts occurring primarily from the loess area, mostly in the spring season, are dispersed and transported because soil dusts are easily transported by the ascending air current, when the dry frozen soil

in winter melts rapidly in the spring. This is coincident with the weakening high atmospheric pressure and the strengthening low atmospheric pressure systems. Therefore, the occurrence, transport, and deposition of Asian dusts are greatly influenced by weather conditions such as atmospheric dryness, precipitation, snowfall, and wind speed in and around the source areas.<sup>17</sup>

The mean mass concentrations ( $n=19$ ) of  $PM_{10}$  and  $PM_{2.5}$  measured in the Gosan site on Jeju Island during Asian dust periods from 2010-2015 were  $130.0 \pm 90.2$  and  $38.2 \pm 24.7 \mu\text{g}/\text{m}^3$ , respectively.  $PM_{10}$  had a higher rate of increase than  $PM_{2.5}$ , showing similar trends to those shown in previous studies.<sup>18,19</sup> These mass concentrations were 3.3 and 2.5 times higher, respectively, than the values of  $39.5 \pm 17.0 \mu\text{g}/\text{m}^3$  in  $PM_{10}$  and  $15.1 \pm 7.4 \mu\text{g}/\text{m}^3$  in  $PM_{2.5}$ , which were measured in the same location on non-event days ( $n=44$ ) in 2014 and reported in a previous study.<sup>15</sup>

The mean concentrations of major ionic species of  $PM_{10}$  and  $PM_{2.5}$  during the Asian dust period are shown in Fig. 2. Here, the concentration of non-sea salt sulfate ions ( $\text{nss-SO}_4^{2-}$ ) was calculated using the formula:  $[\text{nss-SO}_4^{2-}] = [\text{SO}_4^{2-}] - [\text{Na}^+] \times 0.251$ . The concentration of non-sea salt calcium ( $\text{nss-Ca}^{2+}$ ) was calculated using the formula:  $[\text{nss-Ca}^{2+}] = [\text{Ca}^{2+}] - [\text{Na}^+] \times 0.04$ .<sup>20,21</sup>

The fine dust particles ( $PM_{10}$ ) were classified into  $PM_{10-2.5}$  (coarse particle,  $2.5 < D_p < 10 \mu\text{m}$ ) and  $PM_{2.5}$

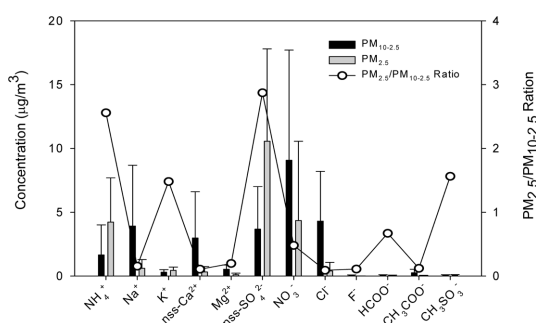


Fig. 2. Concentrations of water-soluble ionic species and their ratios in  $PM_{2.5}$  and  $PM_{10-2.5}$  particles during Asian dust days.

(fine particle,  $D_p < 2.5 \mu\text{m}$ ), and the compositional characteristics of coarse versus fine particles were compared.<sup>22</sup> In general, coarse particles are generated through mechanical processes on the Earth's surface, and their atmospheric residence time is relatively short. However, fine particles have different chemical compositions, as they are produced from chemical reactions arising from anthropogenic activities and gaseous pollutants from fossil fuel combustion.<sup>22,23</sup> The concentrations of each ion species in  $PM_{10-2.5}$  and  $PM_{2.5}$  were compared in order to understand the differences.

The mean concentrations of ionic species of  $PM_{10-2.5}$  coarse particles were in the order of  $\text{NO}_3^- > \text{Cl}^- > \text{Na}^+ > \text{nss-SO}_4^{2-} > \text{nss-Ca}^{2+} > \text{NH}_4^+ > \text{Mg}^{2+} > \text{K}^+ > \text{CH}_3\text{COO}^- > \text{HCOO}^- > \text{F}^- > \text{CH}_3\text{SO}_3^-$ . Of these,  $\text{NO}_3^-$  concentration was  $9.07 \mu\text{g}/\text{m}^3$ , the highest value at

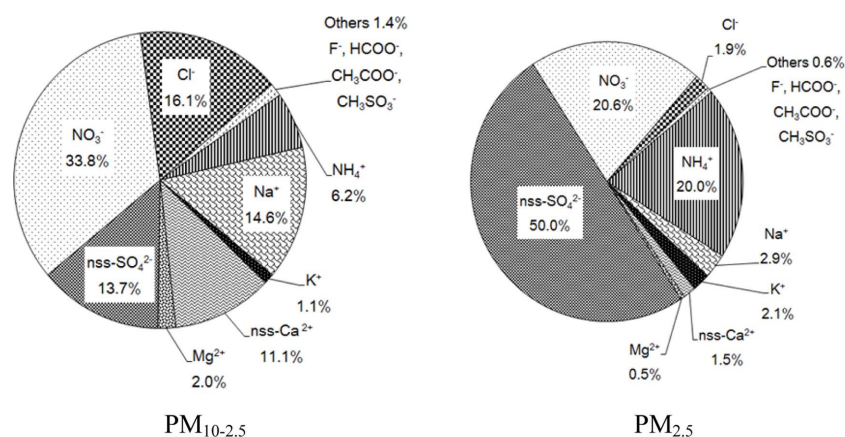


Fig. 3. Composition ratios of water-soluble ionic species in  $PM_{10-2.5}$  and  $PM_{2.5}$  particles during Asian dust days.

the Gosan site. In comparison, the concentration of  $\text{NO}_3^-$  on non-event days in 2014 was  $1.91 \mu\text{g}/\text{m}^3$ ; that is, the concentration of  $\text{NO}_3^-$  species was 3.8 times higher owing to the effect of Asian dust. For the ionic compositions in the  $\text{PM}_{10-2.5}$  mode fraction, the major secondary pollutants ( $\text{nss-SO}_4^{2-}$ ,  $\text{NO}_3^-$ ,  $\text{NH}_4^+$ ) accounted for 53.7 % of the total, followed by the sea salt species ( $\text{Na}^+$ ,  $\text{Cl}^-$ ,  $\text{Mg}^{2+}$ ) at 32.6 %, soil species ( $\text{nss-Ca}^{2+}$ ) at 11.1 %, and organic acid species ( $\text{CH}_3\text{COO}^-$ ,  $\text{HCOO}^-$ ) at 1.2 %. Notably, the concentration of  $\text{nss-Ca}^{2+}$  species originating from soil on Asian dust days was 3.5 times higher than that on the non-event days at the Gosan site in 2014.<sup>15</sup>

In comparison, the mean concentrations of the ionic species in  $\text{PM}_{2.5}$  fine particles were in the following order:  $\text{nss-SO}_4^{2-} > \text{NO}_3^- > \text{NH}_4^+ > \text{Na}^+ > \text{K}^+ > \text{Cl}^- > \text{nss-Ca}^{2+} > \text{Mg}^{2+} > \text{CH}_3\text{SO}_3^- > \text{CH}_3\text{COO}^- > \text{HCOO}^- > \text{F}^-$ . The concentrations of the  $\text{NH}_4^+$  and  $\text{nss-SO}_4^{2-}$  species were  $4.23$  and  $10.56 \mu\text{g}/\text{m}^3$ , respectively, and showed 2.6 times and 2.9 times higher concentrations than in the  $\text{PM}_{10-2.5}$  coarse particles. The concentrations of the  $\text{NO}_3^-$  species in coarse and fine particles during the Asian dust periods were  $9.07$  and  $4.35 \mu\text{g}/\text{m}^3$ , respectively; the coarse particle concentrations were 2.1 times higher than the fine particle concentrations. The concentration of nitrate ions in coarse particles is hypothesized to be higher during Asian dust periods because of a nitrogen oxide chemical reaction on the surface of the particles that results in a salt, such as  $\text{Ca}(\text{NO}_3)_2$ .<sup>24,25</sup> These results in the present study are in agreement with those of other research on Asian dust, which

indicated that the concentration of nitrate in  $\text{PM}_{10}$  and  $\text{PM}_{2.5}$  increased simultaneously with the transport of Asian dust originating from Inner Mongolia.<sup>13,26</sup>

In addition, the secondary pollutants in the  $\text{PM}_{2.5}$  ionic species were very high, accounting for 90.6 %, and were about 1.7 times higher than those in coarse particles (*Fig. 3*). In contrast, the remaining composition included 5.2 % sea salt, 1.5 % soil origin, and 0.3 % organic acid origin. As shown in *Fig. 2*, the concentration ratios ( $\text{PM}_{2.5}/\text{PM}_{10-2.5}$ ) of the ionic species  $\text{NH}_4^+$ ,  $\text{nss-SO}_4^{2-}$ , and  $\text{K}^+$  in  $\text{PM}_{2.5}$  and  $\text{PM}_{10-2.5}$  during Asian dust periods were greater than 1, indicating that these species were mainly distributed in fine particle mode. In contrast, the ionic species  $\text{nss-Ca}^{2+}$ ,  $\text{Na}^+$ ,  $\text{Cl}^-$ ,  $\text{Mg}^{2+}$ , and  $\text{NO}_3^-$  had relatively higher distribution in the coarse particles.

The compositions of elemental species of coarse ( $\text{PM}_{10-2.5}$ ) and fine ( $\text{PM}_{2.5}$ ) particles were compared for Asian dust samples ( $n=11$ ) between 2014 and 2015 (*Figs. 4-5*). The concentrations of elemental species in  $\text{PM}_{10-2.5}$  during the Asian dust periods were in the following order:  $\text{Ca} > \text{Fe} > \text{S} > \text{Na} > \text{Al} > \text{Mg} > \text{K} > \text{Ti} > \text{Zn} > \text{Mn} > \text{Ba} > \text{Pb} > \text{Sr} > \text{Ni} > \text{V} > \text{Cr} > \text{Cu} > \text{Co} > \text{Cd} > \text{Mo}$ . The Ca concentration was  $2425.5 \text{ ng}/\text{m}^3$ , which was the highest concentration, and the concentrations of Fe, S, Na, and Al were similar, ranging from  $2276.7$ - $2329.8 \text{ ng}/\text{m}^3$ . In comparison, the concentrations of the elemental species in  $\text{PM}_{2.5}$  were in the order of  $\text{S} > \text{Al} > \text{Fe} > \text{Ca} > \text{Na} > \text{K} > \text{Mg} > \text{Zn} > \text{Pb} > \text{Ti} > \text{Mn} > \text{V} > \text{Ba} > \text{Ni} > \text{Sr} > \text{Cu} > \text{Cr} > \text{Cd} > \text{Mo} > \text{Co}$ . Of these, S concentration had the highest value,  $3403.4 \text{ ng}/\text{m}^3$ . Notably, the concentrations of Al, Fe, Ca, Na, Mg,

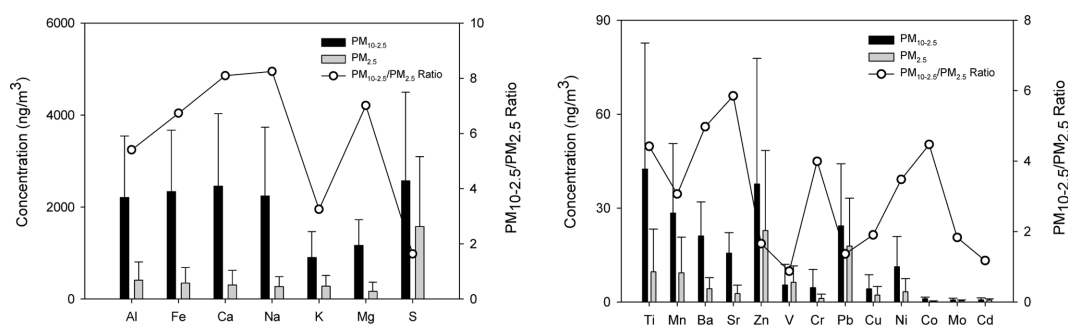


*Fig. 4.* Concentrations of elemental species and their ratios in  $\text{PM}_{10-2.5}$  and  $\text{PM}_{2.5}$  particles during Asian dust days.

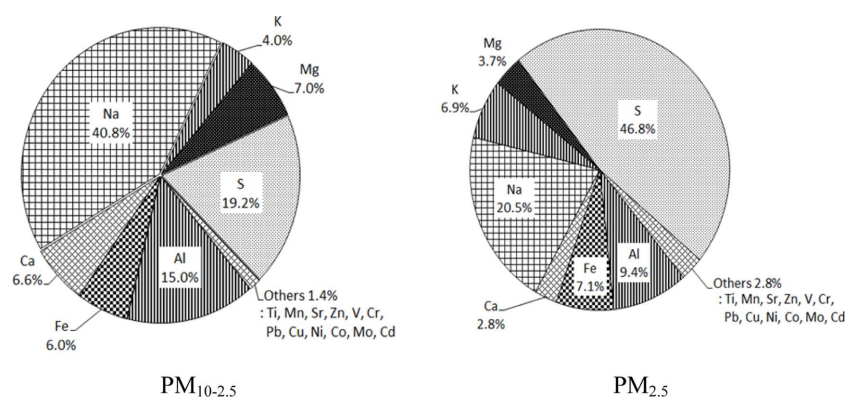


Fig. 5. Composition ratios of elemental species in PM<sub>10-2.5</sub> and PM<sub>2.5</sub> particles during Asian dust days.

Ba, Sr, and Ti were 5.3, 6.5, 7.6, 8.2, 6.7, 4.8, 5.5, and 4.4 times lower in the fine particles than in the coarse particles. In general, among the elemental species, typical crustal materials such as Si, Al, K, Na, Ca, and Fe and trace amounts of Ba, Sr, Rb, and Li are concentrated in coarse particles.<sup>27</sup> However, the concentrations of Ni, Zn, and Pb, which originated mainly from anthropogenic sources, were relatively higher in coarse particles than in fine particles, indicating an increasing pollution effect during Asian dust periods.

In the coarse particles, major soil species (Al, Fe, Ca) showed the highest composition ratio, at 50.5 % of the elemental species, followed by 24.9 % sea salt species (Na, Mg) and 17.2 % anthropogenic origin species (S, Zn, Pb, Ni); however, these composition ratios were 32.6, 13.3, and 45.2 %, respectively, in the fine particles. Species of anthropogenic origin accounted for a relatively high proportion of the total, 45.2 %. In summary, the species derived from soil and sea salt in the coarse particles were, respectively, 1.5 and 1.9 times more concentrated than in the fine particles, yet the anthropogenically derived species in the fine particles were 2.6 times higher than those in the coarse particles (Fig. 5).

### 3.2. Concentration comparison of the chemical species by transport pathways of Asian dust

Asian dusts usually originate at the Loess Plateau as well as the Taklimakan, Ordos, Tengger, Badain Jaran, and Gobi Deserts, which are the major desert

areas in China and Mongolia. The impacts of Asian dust on the Korean peninsula may vary depending on the transport pathways as well as its originations. According to the “Asian dust and smog report in 2015” published by the NIMR of the KMA, 126 Asian dust events affected the Korean peninsula between 2002 and 2015.<sup>10</sup> Furthermore, the transport pathways bringing Asian dust from the Gobi and Inner Mongolia to the Korean peninsula through Bohai Bay (Liaodong Peninsula) accounted for 48 % of deposited dust (60 events). Those originating from the Gobi and Inner Mongolia that were transported to the Korean Peninsula through Manchuria and the Liaodong Peninsula accounted for 18 % of deposited dust (22 events). Asian dust events originating from Inner Mongolia and transported to the Korean Peninsula through the Loess Plateau accounted for 15 % (19 events) of the total, whereas 19 % (22 events) originated in Manchuria and were transported through the Liaodong Peninsula (North Korea). Finally, Asian dust originating from the Loess Plateau and transported to the Korean Peninsula through the Shandong Peninsula accounted for 1 % of the events (1 event).<sup>10</sup>

In this study, an attempt to compare the variations of chemical composition concentrations according to the transport pathways of 12 Asian dust events between 2010 and 2015 was tried. The transport pathways of Asian dust were divided into three parts: northern, central, and southern China, similar to the pathways classified by the KMA. As shown in

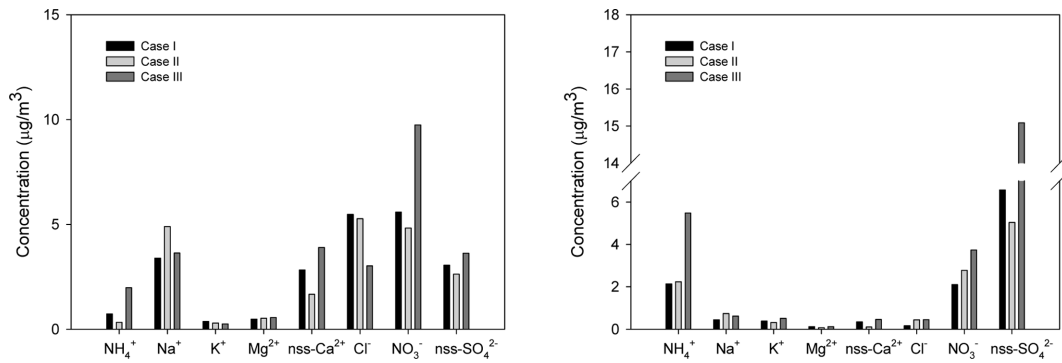


Fig. 6. Concentrations of ionic species in PM<sub>10-2.5</sub> (left) and PM<sub>2.5</sub> (right) in relation to three different inflow pathways of Asian dusts.

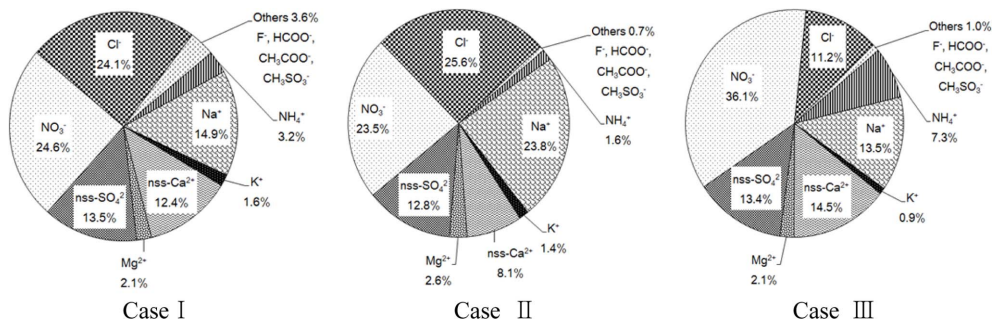


Fig. 7. Composition ratios of ionic species in PM<sub>10-2.5</sub> particle in relation to three different inflow pathways of Asian dusts.

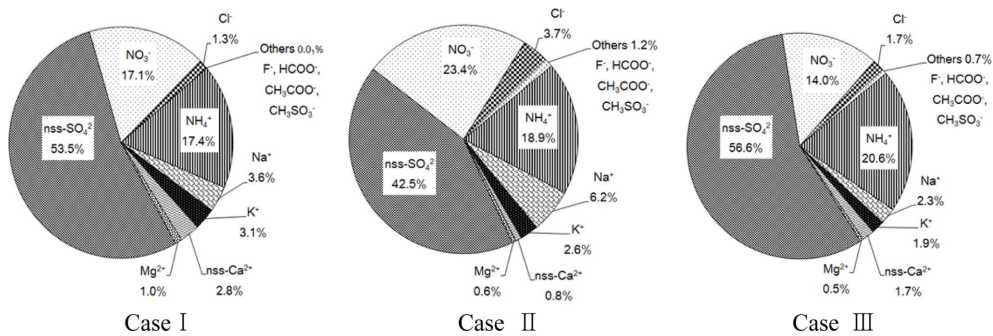


Fig. 8. Composition ratios of ionic species in PM<sub>2.5</sub> particle in relation to three different inflow pathways of Asian dusts.

Fig. 6, the concentrations of Na<sup>+</sup>, Cl<sup>-</sup>, and K<sup>+</sup> in PM<sub>10-2.5</sub> coarse particles were relatively high, 4.89, 5.47, and 0.37 µg/m<sup>3</sup>, respectively, when transported through Manchuria (Case I) and Bohai Bay (Case II). However, when Asian dust was transported through the Loess Plateau (Case III), the concentrations of the nss-Ca<sup>2+</sup>, NH<sub>4</sub><sup>+</sup>, nss-SO<sub>4</sub><sup>2-</sup>, and NO<sub>3</sub><sup>-</sup> species were relatively higher. The concentrations of the nss-Ca<sup>2+</sup>, NH<sub>4</sub><sup>+</sup>, nss-SO<sub>4</sub><sup>2-</sup>, and NO<sub>3</sub><sup>-</sup> species in PM<sub>2.5</sub>

were also high, similar to the case for coarse particles, for Asian dust transported through the Loess Plateau (Case III).

Fig. 7 shows that the sum of the composition ratios of the ionic nss-SO<sub>4</sub><sup>2-</sup>, NO<sub>3</sub><sup>-</sup>, and NH<sub>4</sub><sup>+</sup> species in PM<sub>10-2.5</sub> were 41.2 %, 37.8 %, and 56.9 %, when those major secondary pollutants were transported through Bohai Bay (Case I), Manchuria (Case II), and the Loess Plateau (Case III), respectively.

However, in PM<sub>2.5</sub>, the sum of the composition ratios of the ionic nss-SO<sub>4</sub><sup>2-</sup>, NO<sub>3</sub><sup>-</sup>, and NH<sub>4</sub><sup>+</sup> species were 88.1 %, 84.8 %, and 91.2 %, respectively, as shown in Fig. 8, and the highest composition was achieved when they were transported through the Loess Plateau. The nss-Ca<sup>2+</sup> species in PM<sub>10-2.5</sub> transported through the Loess Plateau accounted for 14.5 %; 1.2 and 1.8 times higher than those through Manchuria and Bohai Bay, respectively. In contrast, Na<sup>+</sup> and Cl<sup>-</sup> in PM<sub>10-2.5</sub> showed a relatively high percentile when transported through Bohai Bay.

Among the elemental species in Asian dust transported through Manchuria and Bohai Bay, the concentrations of soil-derived Fe and Ca species were very high in PM<sub>10-2.5</sub>, at 2842.6 and 3489.4 ng/m<sup>3</sup>, respectively. The concentration of S was 3009.2 ng/m<sup>3</sup> when transported through the Loess Plateau, and the result was that the anthropogenically derived species in Case III showed relatively high concentrations compared to other pathways. For fine particles, the S species showed mostly high concentrations in Case I, Case II, and Case III, at 793.4, 1434.8, and 2410.9 ng/m<sup>3</sup>, respectively. The composition ratios for coarse particles indicated relatively high contributions from soil-derived species (Al, Fe, Ca); 50.0 %, 54.8 %, and 47.1 % for Cases I, II, and III, respectively. The crustal species showed comparatively higher composition ratios in coarse particles. In particular, the species derived from sea salt in Case II and the anthropogenically derived species in Case III (S, Ni, Pb, Zn) had relatively higher composition ratios compared to those of other pathways. On the other hand, the composition ratios of the anthropogenically derived species were high for all pathways of fine particles, and the highest (51.6 %) occurred for transport through the Loess Plateau.

### 3.3. Acidification and neutralization contributions

Sulfur oxides and nitrogen oxides in the atmosphere are converted to sulfuric acid and nitric acid, respectively, through photochemical reactions. They are then distributed in fine dusts in the form of solid sulfate or nitrate produced from neutralization reactions with ammonia or basic materials in soil. Trace

organic acid species are also neutralized with ammonia and calcium carbonate.<sup>28</sup> Therefore, the acidification contribution from SO<sub>4</sub><sup>2-</sup> and NO<sub>3</sub><sup>-</sup> species can be evaluated by measuring their concentrations. For this, the equivalent ionic concentrations categorized by Asian dust transport pathways are compared in Table 3.

The sums of equivalent concentrations of cations and anions during the Asian dust periods were 0.288 and 0.227 μeq/m<sup>3</sup> in coarse particles (PM<sub>10-2.5</sub>), respectively, and 0.266 and 0.292 μeq/m<sup>3</sup> in fine particles (PM<sub>2.5</sub>), showing similar results for both particle categories. When the Asian dusts were transported through Bohai Bay, the sums of equivalent concentrations for cations and anions were 0.146 and 0.135 μeq/m<sup>3</sup> in coarse particles, respectively, and 0.140 and 0.152 μeq/m<sup>3</sup> in fine particles. They 0.336 and 0.327 μeq/m<sup>3</sup> in coarse particles, respectively, and 0.269 and 0.306 μeq/m<sup>3</sup> in fine particles, when transported through Manchuria. Similar results occurred for Case III as well. It is assumed that the fine particle species were mainly acidified by H<sub>2</sub>SO<sub>4</sub> and HNO<sub>3</sub>, given that the sums of the equivalent concentrations of cations and anions in coarse particles and fine particles were similar to each other.

Ammonia and calcium carbonate also contribute to the neutralization of acidic substances. The degree of neutralization from these two substances can be evaluated via the neutralization factors (NFs) using Eqs. (1) and (2) as follows:<sup>29</sup>

$$NF_{NH_4^+} = \frac{[NH_4^+]}{[nss-SO_4^{2-}] + [NO_3^-] + [HCOO^-] + [CH_3COO^-]} \quad (1)$$

$$NF_{nss-Ca^{2+}} = \frac{[nss-Ca^{2+}]}{[nss-SO_4^{2-}] + [NO_3^-] + [HCOO^-] + [CH_3COO^-]} \quad (2)$$

where [nss-SO<sub>4</sub><sup>2-</sup>], [NO<sub>3</sub><sup>-</sup>], [HCOO<sup>-</sup>], [CH<sub>3</sub>COO<sup>-</sup>], [NH<sub>4</sub><sup>+</sup>], and [nss-Ca<sup>2+</sup>] are the equivalent concentrations of each species. As shown in Table 4, the average neutralization factors by ammonia during the Asian dust periods in coarse and fine particles were 0.35 and 0.77, respectively; higher neutralization factors

were observed in fine particles than in coarse particles. In contrast, the average neutralization factors by calcium carbonate in coarse and fine particles were 0.68 and 0.07, respectively; much higher neutralization factors occurred in coarse particles than in fine particles.

The comparison of neutralization factors by Asian dust transport pathways showed that the neutralization factors by ammonia in coarse particles were 0.32, 0.13, and 0.57, respectively, through Manchuria (Case I), Bohai Bay (Case II), and the Loess Plateau (Case III). The neutralization contributions by ammonia in coarse particles were relatively high for Asian dust transport through the Loess Plateau and low through Bohai Bay. Notably, the neutralization factor by calcium carbonate in coarse particles was 0.73 for transport through Manchuria; among all the pathways, this was the highest neutralization contribution. The neutralization factors by ammonia in fine particles were 0.73, 0.82, and 0.82 as transported through Manchuria (Case I), Bohai Bay (Case II), and the Loess Plateau (Case III), respectively, and the neutralization factors by calcium carbonate in fine particles were 0.09, 0.03, and 0.03, respectively,

which are almost negligible. These results confirmed that acidic substances in fine particles were primarily neutralized by ammonia, and that those in coarse particles were primarily neutralized by calcium carbonate. In particular, when Asian dust originated from the Gobi and Inner Mongolia, the neutralization contribution by calcium carbonate in coarse particles was higher after passing through Manchuria. Meanwhile, the neutralization contribution by ammonia in fine particles was higher after passing through Bohai Bay and the Loess Plateau.

Atmospheric ammonia exists in aerosols in the form of  $\text{NH}_4\text{HSO}_4$  or  $(\text{NH}_4)_2\text{SO}_4$  owing to neutralization via sulfuric acid. However,  $\text{NH}_4\text{NO}_3$  is produced when sulfuric acid is insufficient or the concentration of ammonia and nitric acid is high and distributed in aerosols.<sup>30,31</sup> Similarly, the  $\text{nss-SO}_4^{2-}$ ,  $\text{NO}_3^-$ , and  $\text{NH}_4^+$  species exist in atmospheric aerosols in salt form, such as ammonium sulfate or ammonium nitrate. Therefore, the amount of ammonium can be calculated using Eqs. (3) to (6) under the assumption that these species are  $\text{nss-SO}_4^{2-}$ ,  $\text{NO}_3^-$ , and  $\text{NH}_4^+$  salts.<sup>32</sup> In the equations,  $[\text{ex-NH}_4^+]$  is the ammonium concentration subtracted from ammonium sulfate concentration.

Table 3. Comparison between the sums of equivalent concentrations of basic cations and acidic anions in  $\text{PM}_{10-2.5}$  and  $\text{PM}_{2.5}$  particles for three different inflow pathways of Asian dusts

Pathway	$\text{PM}_{10-2.5}$ ( $\mu\text{eq}/\text{m}^3$ )				$\text{PM}_{2.5}$ ( $\mu\text{eq}/\text{m}^3$ )			
	Cation		Anion		Cation		Anion	
Case I	$\text{H}^+$	0.003	$\text{nss-SO}_4^{2-}$	0.105	$\text{H}^+$	0.003	$\text{nss-SO}_4^{2-}$	0.188
	$\text{NH}_4^+$	0.147	$\text{NO}_3^-$	0.209	$\text{NH}_4^+$	0.241	$\text{NO}_3^-$	0.118
	$\text{nss-Ca}^{2+}$	0.145	$\text{HCOO}^-$	0.002	$\text{nss-Ca}^{2+}$	0.016	$\text{HCOO}^-$	0.0000
	$\text{Mg}^{2+}$	0.041	$\text{CH}_3\text{COO}^-$	0.011	$\text{Mg}^{2+}$	0.009	$\text{CH}_3\text{COO}^-$	0.0000
	Total	0.336	Total	0.327	Total	0.269	Total	0.306
Case II	$\text{H}^+$	0.001	$\text{nss-SO}_4^{2-}$	0.055	$\text{H}^+$	0.005	$\text{nss-SO}_4^{2-}$	0.105
	$\text{NH}_4^+$	0.018	$\text{NO}_3^-$	0.078	$\text{NH}_4^+$	0.124	$\text{NO}_3^-$	0.045
	$\text{nss-Ca}^{2+}$	0.084	$\text{HCOO}^-$	0.001	$\text{nss-Ca}^{2+}$	0.005	$\text{HCOO}^-$	0.001
	$\text{Mg}^{2+}$	0.043	$\text{CH}_3\text{COO}^-$	0.001	$\text{Mg}^{2+}$	0.006	$\text{CH}_3\text{COO}^-$	0.001
	Total	0.146	Total	0.135	Total	0.140	Total	0.152
Case III	$\text{H}^+$	0.004	$\text{nss-SO}_4^{2-}$	0.049	$\text{H}^+$	0.009	$\text{nss-SO}_4^{2-}$	0.381
	$\text{NH}_4^+$	0.111	$\text{NO}_3^-$	0.172	$\text{NH}_4^+$	0.346	$\text{NO}_3^-$	0.040
	$\text{nss-Ca}^{2+}$	0.104	$\text{HCOO}^-$	0.001	$\text{nss-Ca}^{2+}$	0.011	$\text{HCOO}^-$	0.001
	$\text{Mg}^{2+}$	0.032	$\text{CH}_3\text{COO}^-$	0.003	$\text{Mg}^{2+}$	0.006	$\text{CH}_3\text{COO}^-$	0.0004
	Total	0.251	Total	0.225	Total	0.372	Total	0.422

$$\begin{aligned} [\text{nss-SO}_4^{2-}]_{\text{eq}} / [\text{NH}_4^+]_{\text{eq}} < 1, [(\text{NH}_4)_2\text{SO}_4] \\ = 1.38[\text{nss-SO}_4^{2-}] \end{aligned} \quad (3)$$

$$\begin{aligned} [\text{nss-SO}_4^{2-}]_{\text{eq}} / [\text{NH}_4^+]_{\text{eq}} > 1, [(\text{NH}_4)_2\text{SO}_4] \\ = 3.67[\text{NH}_4^+] \end{aligned} \quad (4)$$

$$[\text{ex-NH}_4^+] = [\text{NH}_4^+] - 0.27[(\text{NH}_4)_2\text{SO}_4] \quad (5)$$

$$[\text{NH}_4\text{NO}_3] = 4.44[\text{ex-NH}_4^+] \quad (6)$$

As shown in Table 5, the concentrations of  $(\text{NH}_4)_2\text{SO}_4$  were 1.1 and 6.5  $\mu\text{g}/\text{m}^3$ , respectively, in  $\text{PM}_{10-2.5}$  and  $\text{PM}_{2.5}$ , and those of  $\text{NH}_4\text{NO}_3$  were 0.1 and 2.2  $\mu\text{g}/\text{m}^3$ , when Asian dust was transported through Bohai Bay (Case II); that is, ammonium sulfate had a higher concentration than ammonium nitrate did. In contrast, the concentrations of  $(\text{NH}_4)_2\text{SO}_4$  and  $\text{NH}_4\text{NO}_3$  were similar in  $\text{PM}_{10-2.5}$ , and ammonium sulfate concentrations were relatively higher in  $\text{PM}_{2.5}$ , when dust was transported through Manchuria (Case I). These ammonium species showed similar concentrations in  $\text{PM}_{10-2.5}$ , but the amount of ammonium sulfate was much higher in  $\text{PM}_{2.5}$  when the dust was transported through the Loess Plateau (Case III). These results suggest that ammonium salts generally exist in aerosols in the form of ammonium sulfate and ammonium nitrate in  $\text{PM}_{10-2.5}$ , but most are likely converted to the ammonium sulfate form in  $\text{PM}_{2.5}$ .

Table 4. Neutralization factors (NF) by ammonia and calcium carbonate in  $\text{PM}_{10-2.5}$  and  $\text{PM}_{2.5}$  particles for three different inflow pathways of Asian dusts

Pathway	NF <sub>NH<sub>3</sub></sub>		NF <sub>CaCO<sub>3</sub></sub>	
	PM <sub>10-2.5</sub>	PM <sub>2.5</sub>	PM <sub>10-2.5</sub>	PM <sub>2.5</sub>
Case I	0.32	0.73	0.73	0.09
Case II	0.13	0.82	0.57	0.03
Case III	0.57	0.82	0.43	0.03
Mean	0.35	0.77	0.68	0.07

Table 5. Estimated concentrations ( $\mu\text{g}/\text{m}^3$ ) of  $(\text{NH}_4)_2\text{SO}_4$  and  $\text{NH}_4\text{NO}_3$  in  $\text{PM}_{10-2.5}$  and  $\text{PM}_{2.5}$  particles

Species	PM <sub>10-2.5</sub>			PM <sub>2.5</sub>		
	Case I	Case II	Case III	Case I	Case II	Case III
$(\text{NH}_4)_2\text{SO}_4$	5.3	1.1	4.3	11.1	6.5	18.8
$\text{NH}_4\text{NO}_3$	5.4	0.1	3.6	6.1	2.2	1.7

## 4. Conclusions

The comparison of pollution characteristics and chemical composition variations based on transport pathways of Asian dust to the Gosan site on Jeju Island from 2010-2015 can be summarized as follows.

The mass concentrations of  $\text{PM}_{10}$  and  $\text{PM}_{2.5}$  during the Asian dust events were  $130.0 \pm 90.2 \mu\text{g}/\text{m}^3$  and  $38.2 \pm 24.7 \mu\text{g}/\text{m}^3$ , respectively, and the concentrations of the major secondary pollutants ( $\text{nss-SO}_4^{2-}$ ,  $\text{NH}_4^+$ ,  $\text{NO}_3^-$ ) were 53.7 % in  $\text{PM}_{10-2.5}$  and 90.6 % in  $\text{PM}_{2.5}$ . The concentrations of the soil-derived elemental species Al, Fe, Ca, Na, Mg, Ba, Sr, and Ti in  $\text{PM}_{10-2.5}$  were 4.4 – 8.2 times higher than those in  $\text{PM}_{2.5}$ .

The  $\text{nss-Ca}^{2+}$ ,  $\text{NH}_4^+$ ,  $\text{nss-SO}_4^{2-}$ , and  $\text{NO}_3^-$  species showed higher concentrations in both coarse and fine particles when Asian dust was transported through the Loess Plateau. The concentrations of S species were higher in fine particles when dust was transported through the Loess Plateau, and soil-derived Al, Fe and Ca showed relatively higher compositions in coarse particles when transported through Bohai Bay.

Sulfuric acid and nitric acid, primarily, caused the acidification of atmospheric aerosols, and ammonia in  $\text{PM}_{2.5}$  and calcium carbonate in  $\text{PM}_{10-2.5}$  contributed to their subsequent neutralization. For Asian dust originating from Inner Mongolia, the neutralization by calcium carbonate in coarse particles was higher when passing through Manchuria, whereas the neutralization by ammonia in fine particles was higher when passing through Bohai Bay and the Loess Plateau. Ammonium salts were generally in the form of ammonium sulfate and ammonium nitrate in  $\text{PM}_{10-2.5}$ , yet most were likely converted to ammonium sulfate in  $\text{PM}_{2.5}$ .

## Acknowledgements

This work was supported by the Project “PoINT” of Jeju National University in 2015.

## References

1. H. Choi and L. M. Sook, *J. Climate Res.*, **7**(1), 30-54 (2012).
2. H. Choi and Y. H. Zhang, *Atmos. Res.*, **89**, 338-350 (2008).
3. H. Chon, *Res. Environ. Sci.*, **7**(6), 1-11 (1994).
4. N. J. Middleton, *J. Climatol.*, **6**, 183-196 (1986).
5. J. Xuan and I. N. Sokolik, *Atmos. Environ.*, **36**(31), 4863-4876 (2002).
6. J. H. Tsai, K. L. Huang, N. H. Lin, S. J. Chen, T. C. Lin, S. C. Chen, C. C. Lin, S. C. Hsu, and W. Y. Lin, *Aerosol Air Qual. Res.*, **12**, 1105-1115 (2012).
7. T. Y. Tanaka and M. Chiba, *J. Meteorol. Soc. Japan*, **83A**, 255-278 (2005).
8. P. Ginoux, J. M. Prospero, O. Torres, and M. Chin, *Environ. Modelling Software*, **19**, 113-128 (2004).
9. D. G. Streets, F. Yan, M. Chin, T. Diehl, N. Mahowald, M. Schultz, M. Wild, Y. Wu, and C. Yu, *J. Geophys. Res.*, **114**, D00D18 (2009).
10. NIMS (National Institute of Meteorological Sciences, 2015) Yellow sand and Haze occurrence case analysis source book, 184pp.
11. NIER (National Institute of Environmental Research, 2008) Research on the current status of Asian Dust from Mongolia and countermeasures, 189pp.
12. M. Y. Kim, *Magazine of the SAREK*, **35**(4), 16-20 (2006).
13. Y. J. Lee, S. A. Jung, M. R. Jo, S. J. Kim, M. K. Park, J. Y. Ahn, Y. S. Lyu, W. J. Choi, Y. D. Hong, J. S. Han, and J. H. Lim, *J. KOSAE*, **30**(5), 434-448 (2014).
14. NIER(2011) 2010 The Annual report for operating result of air pollution intensive monitoring stations.
15. J. M. Song, J. O. Bu, S. H. Yang, J. Y. Lee, W. H. Kim, and C. H. Kang, *J. KOSAE*, **32**(1), 67-81 (2016).
16. A. Mainey and T. William, Compendium of Methods for the Determination of Inorganic Compounds in Ambient Air: (Chapter IO-3) Chemical Species Analysis of Filter-Collected Suspended Particulate Matter, US Environmental Protection Agency EPA/625/R-96/010a, 1-27, 1999.
17. S. Kim and S. Lee, *J. Kor. Geo. Soc.*, **48**(2), 167-183 (2013).
18. S. M. Park, K. J. Moon, J. S. Park, H. J. Kim, J. Y. Ahn, and J. S. Kim, *J. KOSAE*, **28**(3), 282-293 (2012).
19. G. H. Choi, K. H. Kim, C. H. Kang, and J. H. Lee, *Korean J. Atmos. Environ.*, **19**(1), 45-56 (2003).
20. K. F. Ho, S. C. Lee, C. K. Chan, J. C. Yu, J. C. Chow, and X. H. Yao, *Atmospheric Environ.*, **37**(1), 31-39 (2003).
21. M. Nishikawa, S. Kanamori, N. Kanamori, and T. Mizoguchi, *Sci. Tot. Environ.*, **107**, 13-27 (1991).
22. McMurry, P., M. Shepherd, and J. Vickery (2004) Particulate Matter Science for Policy Makers; a NARSTO Assessment (Chapter 3), Cambridge University Press, U.K.
23. D. R. Hyeon, J. M. Song, K. J. Kim, W. H. Kim, C. H. Kang, and H. J. Ko, *Anal. Sci. Technol.*, **27**(4), 213-222 (2014).
24. R. Rengarajan, A. K. Sudheer, and M. M. Sarin, *Atmos. Res.*, **102**(4), 420-431 (2011).
25. S. A. Shin, J. S. Han, Y. D. Hong, J. Y. Ahn, K. J. Moon, S. J. Lee, and S. D. Kim, *J. KOSAE*, **21**(1), 119-129 (2005).
26. NIER (2013a) A study on the characteristics of the air pollutants at the Korean background regions.
27. A. I. Calvo, C. Alves, A. Castro, V. Pont, A. M. Vicente, and R. Fraile, *Atmos. Res.*, **120-121**, 1-28 (2013).
28. J. H. Seinfeld, and S. N. Pandis (1998) Atmospheric Chemistry and Physics, John Wiley & Sons, New York, U.S.A., 408.
29. J. N. Galloway, and W. C. Keene, *Tellus*, **41B**, 427-443 (1989).
30. H. J. Ko, J. M. Song, J. W. Cha, J. Kim, S. B. Ryoo, and C. H. Kang, *J. KOSAE*, **32**(3), 289-304 (2016).
31. W. P. Robarge, J. T. Walker, R. B. McCulloch, and G. Murray, *Atmos. Environ.*, **36**(10), 1661-1674 (2002).
32. W. Rogula-Kozłowska, K. Klejnowski, P. Rogula-Kopiec, L. Ośródk, E. Krajny, B. Błaszczak, and B. Mathews, *Air Qual. Atmos. Heal.*, **7**(1), 41-58 (2014).